



Article

Processing, Mechanical Characterization, and Electric Discharge Machining of Stir Cast and Spray Forming-Based Al-Si Alloy Reinforced with ZrO₂ Particulate Composites

Raviraj Shetty ¹, Prakash Rao Gurupur ², Jamaluddin Hindi ^{1,*}, Adithya Hegde ¹, Nithesh Naik ¹, Mohammed Sabraz Sabir Ali ¹, Ishwargouda S. Patil ³ and Madhukar Nayak ^{4,*}

¹ Department of Mechanical and Industrial Engineering, Manipal Institute of Technology, Manipal Academy of Higher Education, Manipal 576104, India

² Manipal School of Architecture and Planning, Manipal Academy of Higher Education, Manipal 576104, India

³ Department of Mechanical Engineering, National Institute of Technology, Surathkal 575025, India

⁴ Department of Mechanical Engineering, Shri MadhwaVadiraja Institute of Technology and Management, Bantakal 574115, India

* Correspondence: jamaluddin.hindi@manipal.edu (J.H.); madhukarnayaka@gmail.com (M.N.)



Citation: Shetty, R.; Gurupur, P.R.; Hindi, J.; Hegde, A.; Naik, N.; Ali, M.S.S.; Patil, I.S.; Nayak, M. Processing, Mechanical Characterization, and Electric Discharge Machining of Stir Cast and Spray Forming-Based Al-Si Alloy Reinforced with ZrO₂ Particulate Composites. *J. Compos. Sci.* **2022**, *6*, 323. <https://doi.org/10.3390/jcs6110323>

Academic Editor: Francesco Tornabene

Received: 16 September 2022

Accepted: 13 October 2022

Published: 26 October 2022

Publisher's Note: MDPI stays neutral with regard to jurisdictional claims in published maps and institutional affiliations.



Copyright: © 2022 by the authors. Licensee MDPI, Basel, Switzerland. This article is an open access article distributed under the terms and conditions of the Creative Commons Attribution (CC BY) license (<https://creativecommons.org/licenses/by/4.0/>).

Abstract: High performance lightweight structures made of metal matrix composites (MMCs) are in demand for application in variety of industries such as aircraft, spacecraft, automobile, marine, sports equipment, etc. However, uniform distribution of the reinforcement phase to improve the mechanical properties and quality of MMCs has been the challenge for the manufacturing industries. Hence, researchers are focusing on the development of traditional low-cost method of producing metal matrix composites. In the view of above facts, an attempt is made to study the processing and characterization of Si-Al alloy reinforced with zirconium dioxide particulate composites in this paper. Hence, this paper concentrates on experimentally identifying the effect of stir cast and spray forming processing techniques followed by hot pressing on micro hardness, compressive strength, and tensile strength using Taguchi's design of experiments for aluminum silicon matrix alloy reinforced with zirconium dioxide particulates. From the extensive experimentation on aluminum and silicon reinforced with the ZrO₂ powder particulates, it was observed that there was an improvement in selected mechanical properties as the percentage of ZrO₂ increased with 13 wt.% of silicon under spray forming processing technique compared to stir cast composites. This may be due to uniform distribution homogenous dispersion, larger work hardening rate, and structure of dislocation tangles around the ZrO₂ particulates that occurred during spray forming processing technique. Further, results obtained from the interaction plot, contour plot, main effects plot, and analysis of variance (ANOVA) proved to be successful for identifying the optimum processing parameters for Si-Al alloy reinforced with zirconium dioxide particulate composites. Further, this paper also discusses wear study using pin on disc wear testing apparatus on spray forming processed aluminum and silicon (13.0 wt.%) alloy reinforced with the ZrO₂ powder particulates based on Taguchi's design of experiments followed by second order model generation for wear using response surface methodology. Finally, electrode wear study of spray forming processed aluminum and silicon alloy reinforced with the ZrO₂ powder particulates using electric discharge machining by varying peak current (A), pulse on time (μs), and pulse off time (μs) using brass, copper, and graphite as electrode material based on L₂₇ orthogonal array. The understanding gained from the design of experiments in this paper can be used to develop future guidelines for processing and characterization of Si-Al alloy reinforced with zirconium dioxide particulate composites.

Keywords: Si-Al alloy reinforced with zirconium dioxide particulate composites; characterization; design of experiments; orthogonal array; wear

1. Introduction

Modern composite materials have evolved due to the persistent demands of modern technology for high performance materials working under adverse conditions. The processing of composite materials began in the early 1980s, with the development of fiber reinforced plastics (FRP), and advanced into more challenging field of materials such as metallic matrix composites (MMCs) and ceramic matrix composites (CMCs) about three decades ago. Researchers have fabricated aluminum metal matrix composites reinforced with zirconium dioxide and graphite using the stir casting technique. They concluded that zirconium dioxide weight percentage, micro hardness, and compressive strength increased [1]. Aluminum nanocomposites reinforced with zirconium dioxide particulates were fabricated using solution combustion technique. It was concluded that increase in ZrO_2 wt.% caused an increase in hardness of the composite. Further, oxidation, micro cutting, and thermal softening were found to be predominant wear mechanisms during sliding wear conditions [2]. Alumina metal matrix composite with 5, 10, 15 wt.% of zirconia as a reinforced material was manufactured using powder metallurgy technique. They concluded that incorporation of ultra-nano zirconia particulates into aluminum matrix leads to increase in mechanical and electrical properties of aluminum metal matrix composite [3]. Studies have concentrated on physical, mechanical, and tribological characterization of Al6061 alloy reinforced with nano-sized zirconium dioxide particulates fabricated using liquid metallurgy technique. They concluded that in all MMCs, the wear rate increased as the sliding distance and applied stress increased [4]. Ti- ZrO_2 nanocomposites were produced through the powder metallurgical route. It was observed that the “relative density increased with increase in weight fraction of ZrO_2 particulates”. Further, they concluded that “increasing amount of ZrO_2 promoted high hardness in the composite” [5]. Ref. [6] in their research work fabricated Al6061/ ZrO_2 composites using the stir casting technique. They found continuous passive layer deposition on the surface of 3 wt.% ZrO_2 during “immersion in NaCl and the insulated nature of ZrO_2 ceramic particulates” resulted in “high corrosion resistance for prolonged immersion time”. Ref. [7], in their experiment, fabricated aluminum-based metal matrix composite using the stir casting process. They also studied about tribological behavior of the MMCs and performed dry sliding wear test using pin-on-disc method. They suggested that addition of ZrO_2 improves the characteristics of MMC, and the weight percentage can be optimized to improve the behavior of the material for specific applications requiring high strength and wear behavior. Ref. [8] fabricated MMCs with zircon reinforcement using stir casting and squeeze casting. They observed that “abrasive wear resistance of the composite was found to improve significantly with increase in amount of zircon as well as a decrease in the size of zircon particle”. In this experiment, fabrication of zirconia-dispersed aluminum alloy metal matrix composites was produced by stir casting with Aluminum-based composites with varying amounts of 0, 3, 6, 9, and 12 wt.% of zirconia particulates. They observed that the fabricated aluminum LM6 with 12 wt.% of ZrO_2 composite showed a better wear rate and efficiency in performance [9]. Ref. [10] conducted their research on Al6061-zirconium dioxide particulate composites, produced by liquid metallurgy technique with different (2, 4, 6, 8, 10) wt.% of reinforcements. They observed that 2 wt.% of ZrO_2 showed reasonably high strength and hardness when compared to matrix alloy. Al6061- ZrO_2 wt.% composites were manufactured through stir casting technique for 0, 3, 6, 9, and 12 wt.% of zirconium dioxide. They observed that the hardness increased with addition of ZrO_2 up to 9% wt.% and decreased with addition of 12 wt.% of ZrO_2 as reinforcements. Further the optimum value of BHN was obtained at 9 wt.% of zirconia [11]. In an experiment, fabrication of aluminum reinforced by aluminum nitride, silicon nitride, and zirconium dioxide boride particulates was conducted varying wt.% using the stir casting method. They observed an increase in strength and hardness of the composite [12]. The purpose of this research was to determine the wear behavior of aluminum hybrid metal matrix composites fabricated using the squeeze casting technique. During processing, zirconium dioxide (6 wt.%) and graphite (3 wt.%), respectively, were added as reinforcements. They suggested that squeeze

casting process input parameters such as squeeze pressure, molten metal temperature, and die temperature had a major effect on wear behavior of composites followed by weight percentage [13]. Ref. [14] used RSM for Al7075 reinforced with 3 wt.%, 6 wt.%, 9 wt.% silicon carbide particulates, and 1 wt.% of molybdenum disulfide. Through RSM, it was found that Al7075 + 9% SiC + 1% MoS₂ gave the optimum tensile strength and hardness values. In an experiment, Al-Al₂O₃ MMCs were machined using EDM using L9 orthogonal array. It was observed that MRR decreases with increase in volume fraction of reinforcements due to decrease in electrical conductivity [15]. In a study, electrode wear model of electric discharge drilling was developed. From the model generated, the electrode wear can be effectively used as wear estimation models during experimentation [16]. Another study focused on wear study of tungsten electrodes during electro discharge drilling of stainless steel by varying process input parameters. They concluded that electrode wear increases as the current limiting resistance decreases [17]. In their research, they observed that material deposit at the edges of electrode resulted in increase of electrode mass. “The volume and number of applications of composite materials have grown steadily, penetrating and conquering new markets relentlessly”. Currently, material scientists around the world are engaged in the synthesis of new class of composite materials and processes that improve the mechanical properties and quality of products. Therefore, the influence of weight percentage of zirconium dioxide particulate and different process parameters during spray forming on the microstructure and mechanical property of Si-Al alloy reinforced with zirconium dioxide particulate composites has been investigated in the present paper. Finally, electrode wear analysis during EDM of Si-Al (13 wt.% Si) alloy reinforced with zirconium dioxide particulate composites will be investigated.

2. Experimental

Si-Al alloy matrix with 10 wt.%, 11 wt.%, 12 wt.%, and 13 wt.% silicon reinforced with 0 wt.%, 5 wt.%, 10 wt.%, and 15 wt.% of ZrO₂ particulates of mean diameter 25 μm (Table 1) were processed through spray forming techniques and stir casting. Figure 1 shows the SEM image of Si-Al alloy matrix reinforced with ZrO₂ particulates.

In stir casting, the pouring temperature is kept at 700–710 °C, stirring rate is 200 rpm to produce 50 mm diameter cylindrical bars. Figure 2 shows the stir casting set up. In the spray forming technique, Si-Al alloy matrix with 10 wt. %, 11 wt.%, 12 wt.%, and 13 wt.% silicon is heated in an induction furnace for 850 °C where nitrogen is used as inert gas. The ZrO₂ particulates then enter through atomization chamber at a pressure of 4.5 MPa, holding time of 30 min, and flight distance of 400 mm in the form of droplets and get sprayed to molten form of Si-Al alloy matrix and becomesolidified. Figure 3 shows the spray forming set up.

Then, the specimens were hot pressed for eight hours temperature of 480 °C and a pressure of 55 Mpa using a hydraulic hot press machine. Figure 3 illustrates the hydraulic hot press machine.

Table 1. Chemical composition of zirconium dioxide reinforced with aluminum silicon alloy.

Elements	Wt.%
Si	10.0 to 13.0
Fe	0.18
Mn	0.005
Mg	0.006
Zn	0.017
Pb	0.004
ZrO ₂	0 to 15.0
Al	Balance

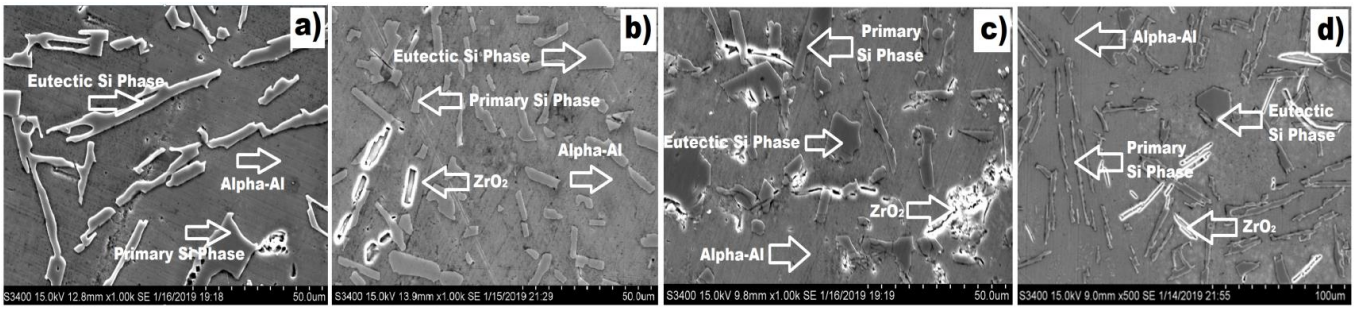


Figure 1. SEM image of Si-Al alloy matrix reinforced with (a) 0% (b) 5%, (c) 10% (d) 15 wt.% of ZrO_2 particulates of mean diameter 25 μm .

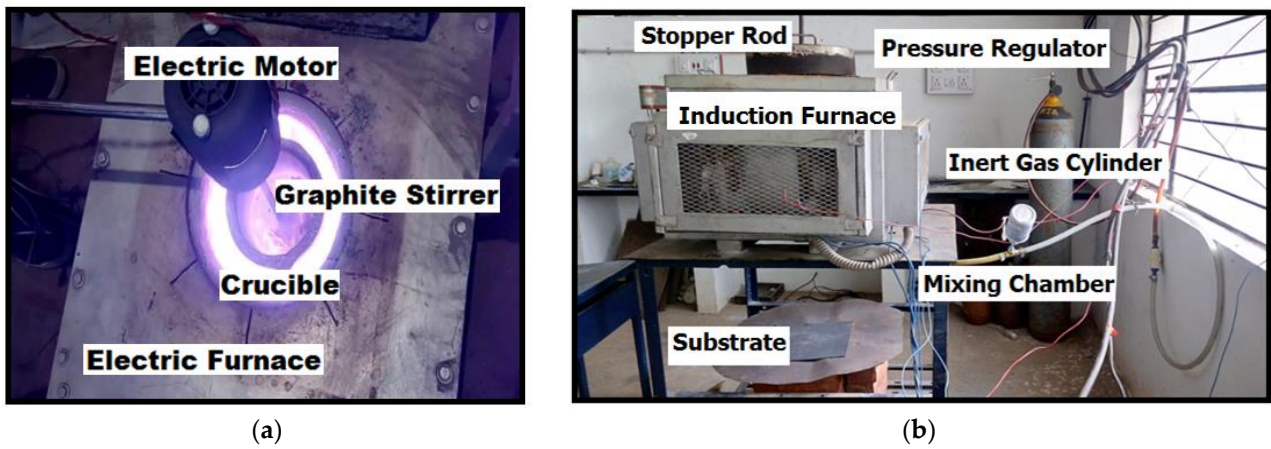


Figure 2. (a) Stir casting set up. (b) Spray forming setup.



Figure 3. Hydraulic hot press machine.

The Matsuzawa micro-hardness testing machine is used for measuring Vickers hardness of the Si-Al- ZrO_2 composite specimens where average micro hardness of the five readings of the composite specimen was taken. The compressive strength (MPa) along with tensile strength (MPa) of the specimen were measured as per ASTM E8, employing Universal Testing Machine (Instron 3366) where average tensile and compressive strength of the three readings were taken. Figures 4 and 5 illustrate the specimens used for research as per ASTM standards.

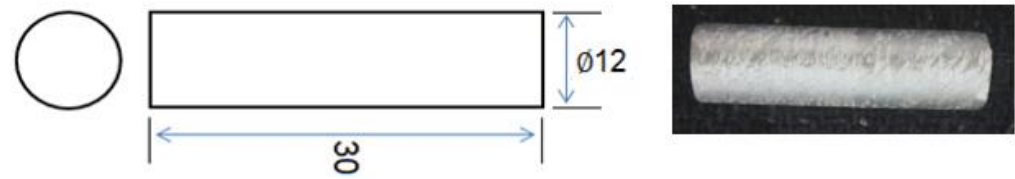


Figure 4. Compression test sample.



Figure 5. Tensile test samples.

The Taguchi’s design of experiments method is the statistical tool used to optimize the processing conditions by formulating the experimental layout by using the software known as MINITAB 15 [18–23]. The *S/N* ratio characteristic (the larger the better) is given in Equation (1).

$$\frac{S}{N} = -\log \frac{1}{n} \left(\sum \frac{1}{y^2} \right) \tag{1}$$

where *n* is the number of observations and *y* is the observed data. In the present work, Taguchi L_{32} orthogonal array is employed to identify the optimal processing conditions. The factors and levels chosen for the experiments are summarized in Table 2.

Table 2. Selected levels and factors.

Levels	(A) Processing Technique	(B) Silicon (wt.%)	(C) Zirconium Dioxide (wt.%)
1	Stir cast	10	0
2	Spray forming	11	5
3	Stir cast	12	10
4	Spray forming	13	15

Two body wear tests were carried out using a pin-on-disc wear testing machine as shown in Figure 6. The pin material was Si-Al (13 wt.%) alloy reinforced with zirconium dioxide particulate composites. Wear rate was characterized as the ratio of loss of mass of workpiece specimen. Aluminum silicon (13 wt.% Si) alloy reinforced with 5, 10, and 15 wt.% ZrO_2 particulate under various parameters such as load (N) and sliding speed (m/s) based on Taguchi’s design of experiments are illustrated in Table 3, followed by mathematical model using response surface methodology (Table 4). Microstructural analysis on worn specimens was conducted using a trinocular inverted metallurgical microscope.

The electric discharge machining experiments on Si-Al (13 wt.%) alloy reinforced with zirconium dioxide particulate composites (cylindrical specimen size of 20 mm thickness, 20 mm dia) with 5 mm dia copper, brass, and graphite electrodes (Figure 7) were carried out using V3525, VM Engineers electric discharge machine as shown in Figure 8.

In the present study of electric discharge machining operation, five parameters, electrode material, peak current (A), pulse on time (μs), pulse off time (μs), and ZrO_2 (wt.%) were identified for machining a 5 mm depth hole. Each parameter was investigated at three levels to study the non-linearity effect of the process parameters. The identified control factors and their levels for TDOE are given in Table 5.

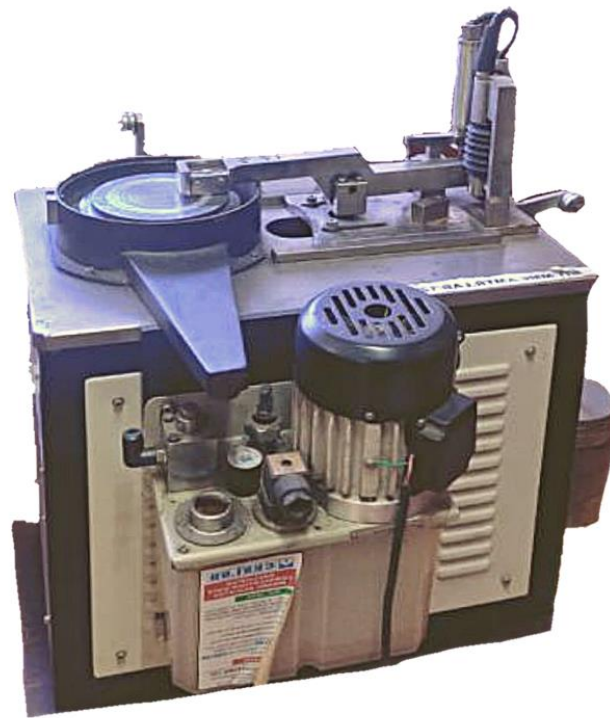


Figure 6. Experimental setup of pin-on-disc wear tester.

Table 3. Selected levels and factors (TDOE).

Levels	(A) Zirconium Dioxide (wt.%)	(B) Load (N)	(C) Sliding Speed (m/s)
1	5	19.62	1.67
2	10	39.24	2.51
3	15	58.86	3.35

Table 4. Selected levels and factors (RSM).

Levels	(A) Zirconium Dioxide (wt.%)	(B) Load (N)	(C) Sliding Speed (m/s)
1	5	19.62	1.67
2	15	58.86	3.35



Figure 7. Electrodematerials: (a) brass, (b) copper, and (c) graphite.



Figure 8. Electric discharge machining set up.

Table 5. Selected levels and factors (TDOE).

Levels	(A) Electrode Material	(B) Peak Current (A)	(C) Pulse on Time (μ s)	(D) Pulse off Time (μ s)	(E) SiC (wt.%)
1	Brass	8	100	50	5
2	Copper	10	200	100	10
3	Graphite	12	300	150	15

3. Results and Discussions

Aluminum-silicon matrix alloy reinforced with zirconium dioxide particulates was manufactured using stir casting and spray forming processing techniques followed by hot press to improve its micro hardness, compressive strength and tensile strength, wear, and machinability, based on Taguchi's design of experiments followed by response surface methodology. Results of the experimentation are discussed in the following subsections.

3.1. Micro Hardness

Figure 9 illustrates the experimentally determined micro hardness values for stir casted and spray formed composites with increasing weight percentages of silicon and ZrO_2 particulates. From the graph, it can be seen that for stir casted and spray formed composites, the micro hardness value increased linearly up to 10 wt.% of ZrO_2 particulates before starting to decrease. This tendency was consistently seen as the weight percentages of silicon and ZrO_2 increased. As a result of ZrO_2 particulates acting as a barrier to dislocation movement in aluminum matrix, it is apparent that, as the number of hard ZrO_2 particulates increases, the hardness of the Al matrix increases. Therefore, the density of dislocations and barriers will increase as ZrO_2 particle numbers increase. Furthermore, when compared to stir casting processes, in the spray forming technique, consistent distribution and homogenous dispersion of ZrO_2 articles leads in an increase in micro hardness values. Thus, we conclude that Al alloy matrix, (13 wt.% Si) reinforced with 10 wt.% of ZrO_2 particulates using the spray forming technique is the optimum parameter for obtaining larger micro hardness value in the composite.

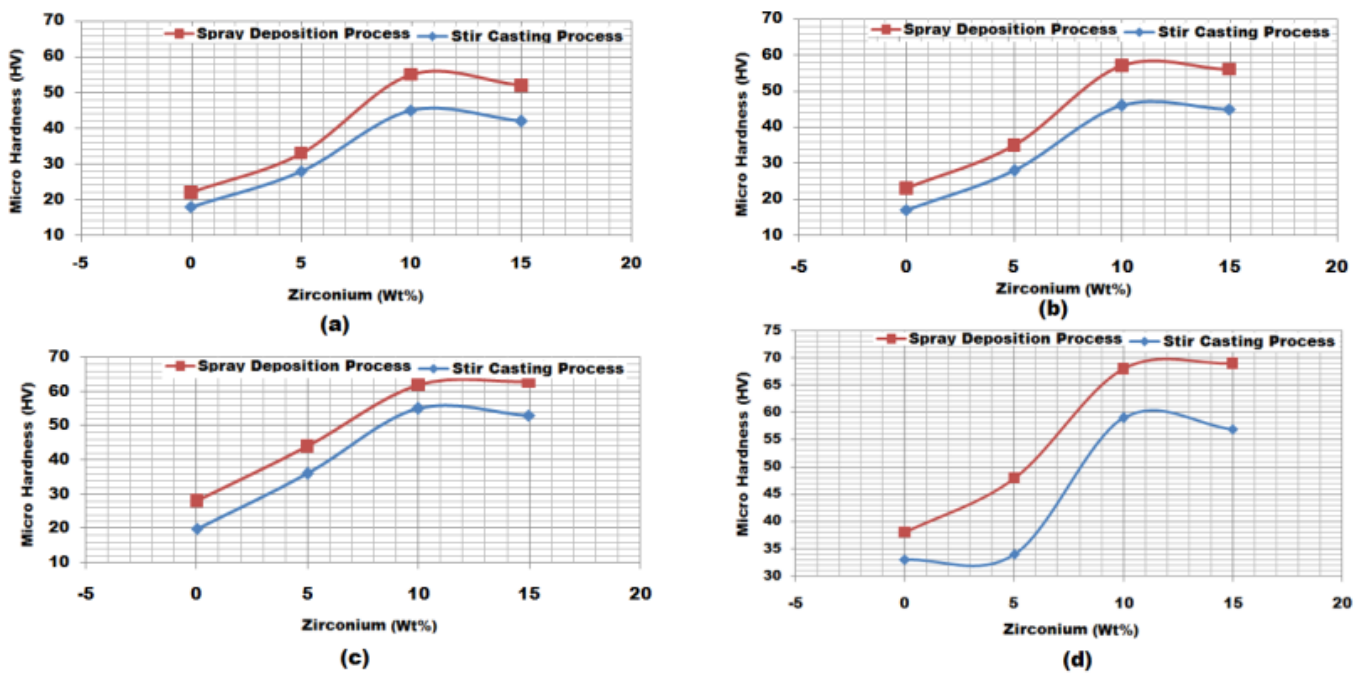


Figure 9. Micro hardness (0.05% error) experimental graph at different processing techniques of Si-Al alloy matrix reinforced with ZrO_2 particulates for (a) 10% (b) 11% (c) 12% (d) 13 wt.% of silicon.

Figure 10 illustrates the micro hardness interaction plot obtained from Taguchi’s design of experiments for stir cast and spray formed Si-Al alloy matrix reinforced with ZrO_2 particulates for 13 wt.% Si. From the interaction plot, similar observations are obtained for stir cast and spray formed composites.

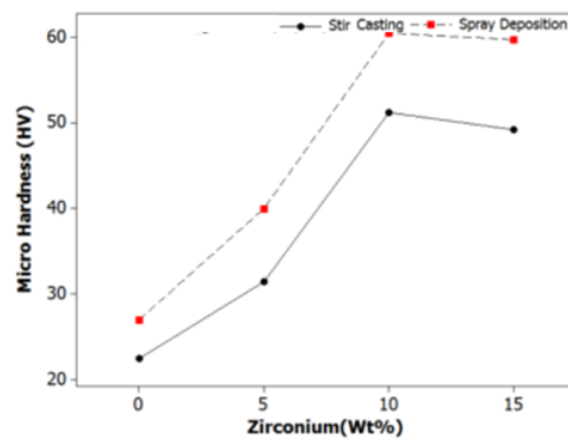


Figure 10. Micro hardness interaction plot at different processing techniques of Si-Al alloy matrix reinforced with ZrO_2 particulates for 13 wt.% Si.

Figure 11 clearly shows that wt.% of ZrO_2 particulates increase from 10 wt.% to 15 wt.% and silicon from 12 wt.% to 13 wt.% resulted in the highest value of micro hardness.

From the main effects graphs (Figure 12) for micro hardness, the optimum processing conditions for obtaining maximum micro hardness can be established at: processing technique (A): spray forming, silicon wt.% (B): 13 wt.%, zirconium dioxide wt.% (C): 10 wt.%.

From analysis of variance (ANOVA), we obtained through Taguchi DOE the percentage contribution (P%) of various selected parameters (Table 6) for micro hardness. Hence, for zirconium dioxide (P% = 62.82%), silicon (P% = 22.06%), and processing technique (P% = 14.18%). Hence, from ANOVA, it can be concluded that zirconium dioxide had the highest contribution towards micro hardness. Figure 13 shows the images of micro hardness test specimens.

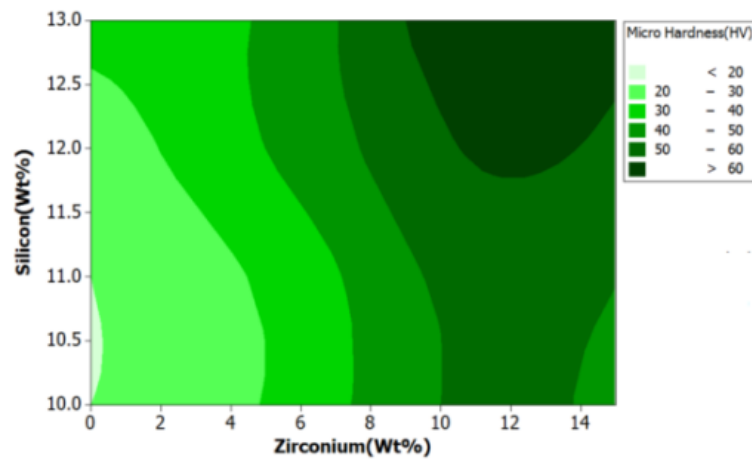


Figure 11. Micro hardness contour plot.

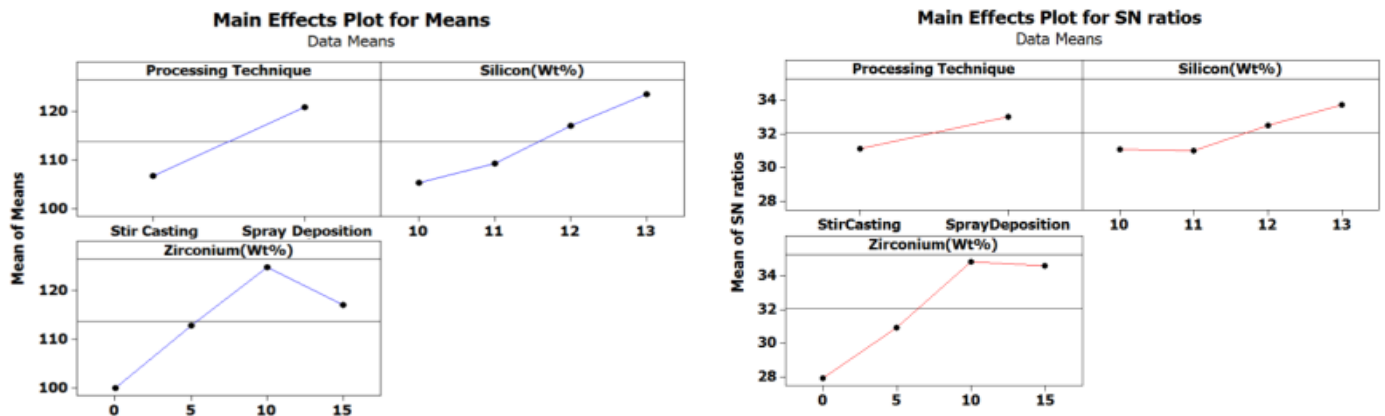


Figure 12. Main effects plot for micro hardness.

Table 6. ANOVA for SN ratios.

Source	DF	Seq SS	Adj SS	Adj MS	F	P	P (%)
(A) Processing technique	1	23.39	23.39	23.39	174.9	0.00	14.18
(B) Silicon (wt.%)	3	109.1	109.1	36.38	272.0	0.00	22.06
(C) Zirconium dioxide (wt.%)	3	310.8	310.8	103.61	774.7	0.00	62.82
AXB	3	0.754	0.754	0.251	1.88	0.20	0.16
AXC	3	1.704	1.704	0.568	4.25	0.04	0.35
BXC	9	6.368	6.368	0.708	5.29	0.01	0.43
Residual error	9	1.204	1.204	0.134			
Total	31	453.4					

3.2. Compressive Strength

Figure 14 illustrates the effect of ZrO₂ wt.% and silicon wt.% on the compressive strength during spray forming and stir casting. From the figure, it was observed that addition of up to 5 wt.% ZrO₂ to aluminum-silicon alloy increases the compressive strength of the composite due to dispersive strengthening mechanism which prevents dislocation movement.

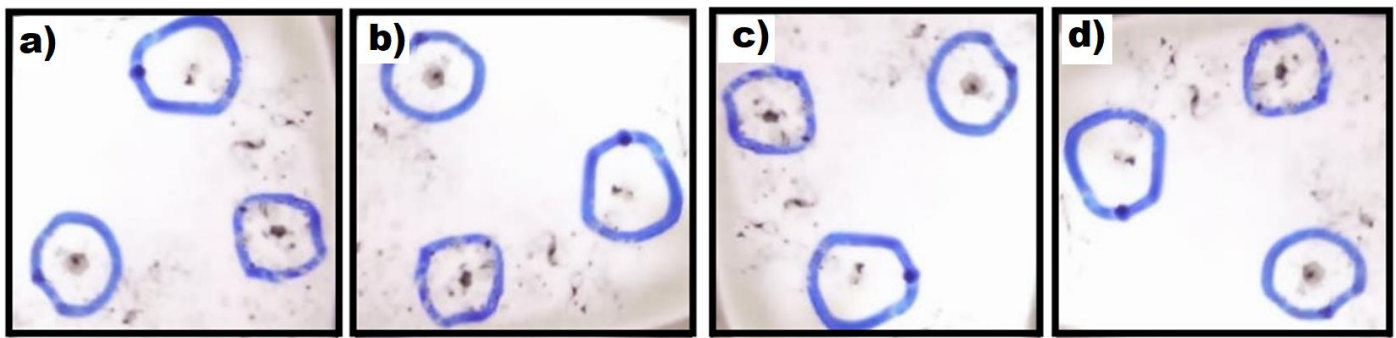


Figure 13. Images of indentations on micro hardness test specimens with (a) 0% (b) 5% (c) 10% (d) 15% ZrO₂ particulates reinforced with 13 wt.% Si.

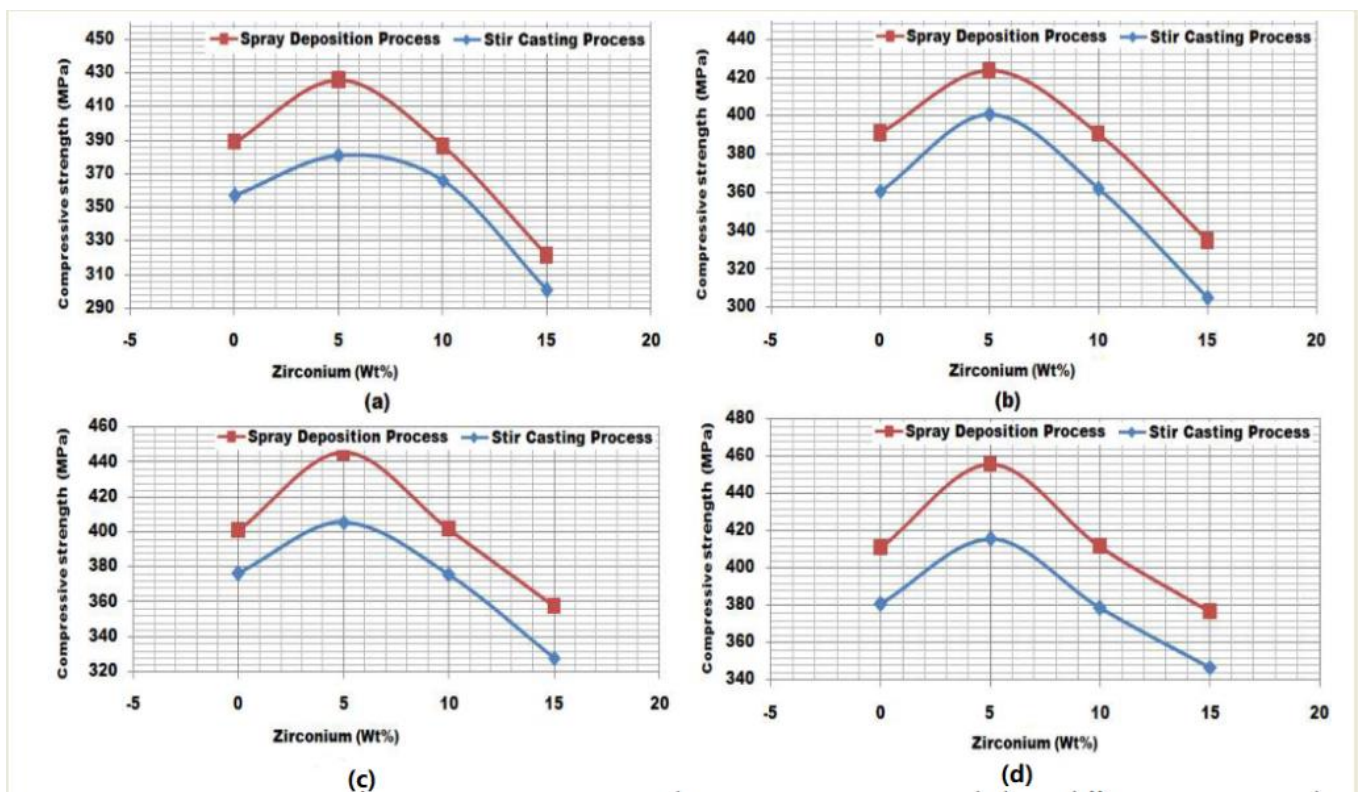


Figure 14. Compressive strength (0.05% error) experimental plot at different processing techniques of Si-Al alloy matrix reinforced with ZrO₂ particulates for (a) 10% (b) 11% (c) 12% (d) 13 wt.% Si.

From Figure 15 (compressive strength interaction plot), it can be observed that 5 wt.% of ZrO₂ particulates resulted in maximum compression strength value while processing under spray forming technique.

Figure 16 shows the contour plot of compressive strength at zirconium dioxide–silicon planes of Si-Al alloy matrix reinforced with ZrO₂ particulates manufactured under spray forming processing techniques. From the contour plot, maximum compressive strength value results from increase of ZrO₂ particulates from 1.75 wt.% to 6 wt.% and silicon from 11.5 wt.% to 13 wt.%.

From the main effects plot in Figure 17 for compressive strength, the optimum processing conditions for the compressive strength can be established at: processing technique (A): spray forming, silicon wt.% (B): 13 wt.%, zirconium dioxide wt.% (C): 5 wt.%.

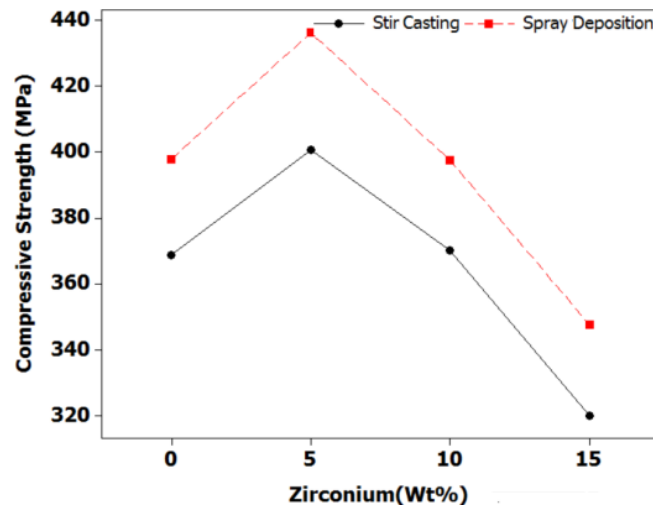


Figure 15. Compressive strength interaction plot.

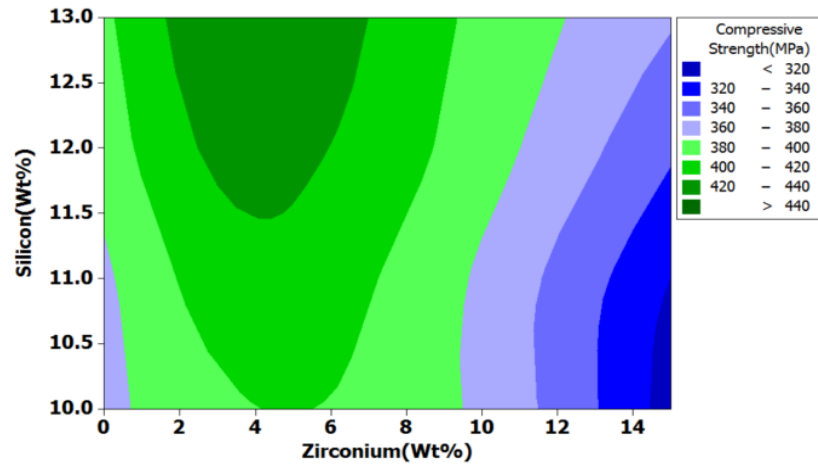


Figure 16. Compressive strength contour plot.

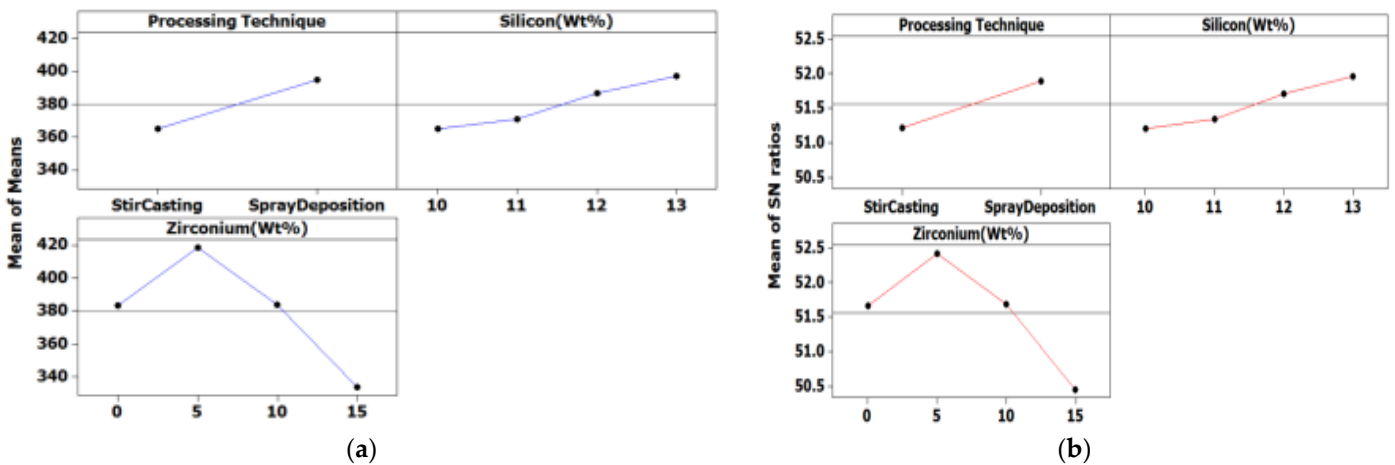


Figure 17. Main effects plot for (a) means and (b) SN ratio for compressive strength.

Table 7 shows the ANOVA results for compressive strength. Hence, from ANOVA for percentage of contribution (P%), it can be seen that zirconium dioxide 50.0%, silicon 9.9%, and processing technique 39.3%. Figure 18 illustrates the images of compressive strength test specimens.

Table 7. ANOVA for SN ratios.

Source	DF	Seq SS	Adj SS	Adj MS	F	P	P (%)
(A) Processing technique	1	3.726	3.726	3.726	410.7	0.00	39.3
(B) Silicon (wt.%)	3	2.827	2.827	0.9425	103.8	0.00	9.9
(C) Zirconium dioxide (wt.%)	3	16.01	16.01	5.3395	588.5	0.00	50.0
AXB	3	0.005	0.005	0.0017	0.20	0.89	0.02
AXC	3	0.017	0.017	0.0058	0.64	0.60	0.05
BXC	9	0.570	0.570	0.0633	6.98	0.00	0.61
Residual error	9	0.081	0.081	0.0090			
Total	31	23.24					

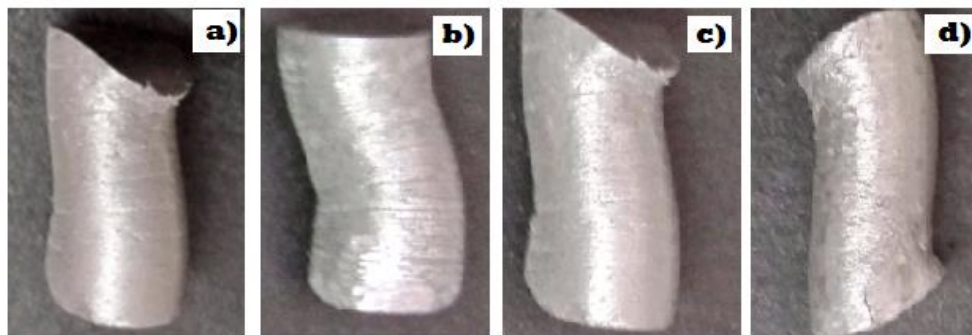


Figure 18. Images of compressive strength test specimens having (a) 0% (b) 5% (c) 10% (d) 15% ZrO₂ particulates for 13 wt.% Si.

3.3. Tensile Strength

Figure 19 shows the tensile test results of Si-Al alloys reinforced with ZrO₂ powder particulates (0 wt.%, 5.0 wt.%, 10.0 wt.%, 15.0 wt.%). The result reveals that the tensile strength of the composite increases with increase in the ZrO₂ particle wt.%. However, for spray forming processed composites, 15 wt.% of ZrO₂ particulates and 13 wt.% silicon the tensile strength value increased to 139.87 MPa. This may be due to larger strain hardening, dislocation tangles, homogenous distribution of particulates, grain refinement, and plastic incongruity.

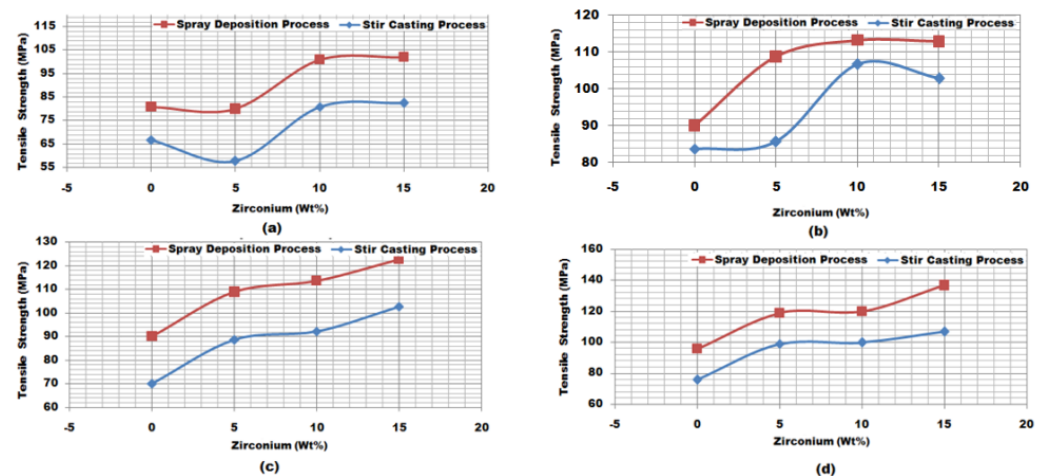


Figure 19. Tensile strength (0.05% error) experimental plot at different processing techniques of Si-Al alloy matrix reinforced with ZrO₂ particulates for (a) 10% (b) 11% (c) 12% (d) 13 wt.% Si.

From Figure 20, it was observed that 15 wt.% of ZrO₂ gave the maximum tensile strength value under the spray forming processing technique and silicon (13 wt.%) resulted in maximum tensile strength value under the spray forming technique. Figure 21 illustrates Tensile strength contour plot at zirconium dioxide–silicon planes.

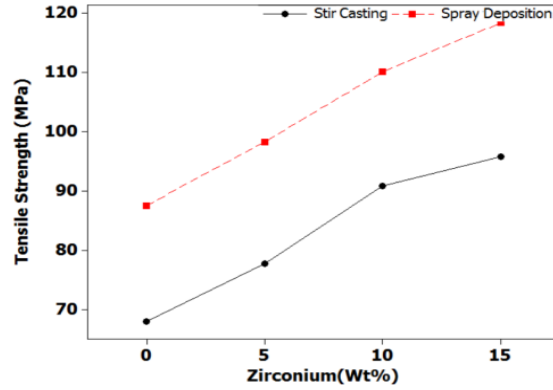


Figure 20. Tensile strength interaction plot.

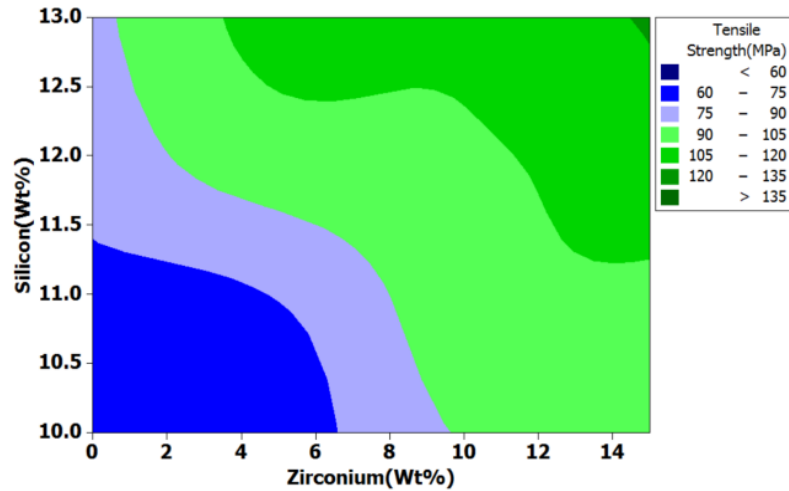


Figure 21. Tensile strength contour plot at zirconium dioxide–silicon planes.

From the main effects plot Figure 22 for tensile strength, the optimum processing conditions for the tensile strength can be established at processing technique (A): spray forming, silicon wt.% (B): 13 wt.%, zirconium dioxide wt.% (C): 15 wt.%.

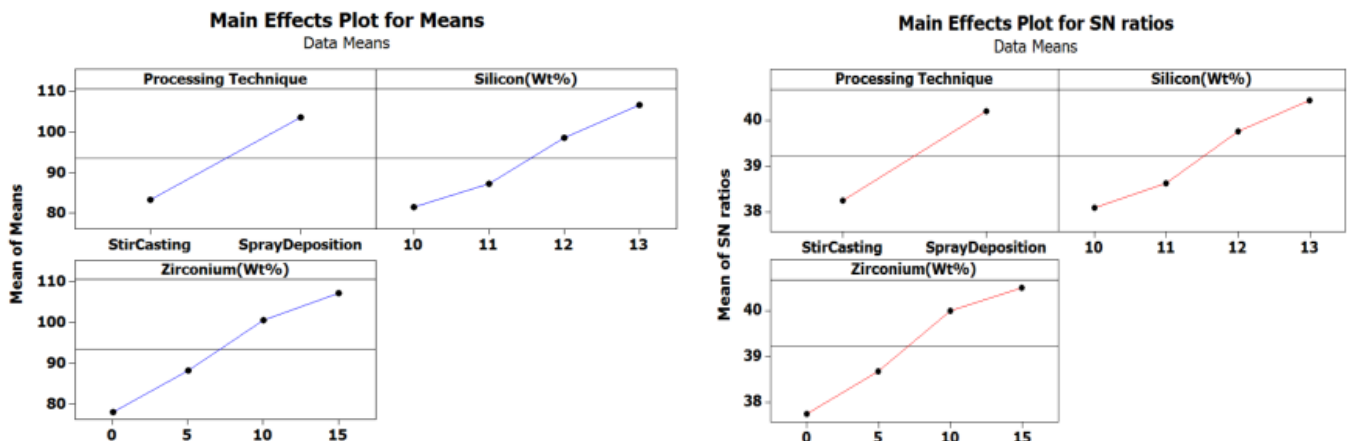


Figure 22. Main effects plot for means and SN ratio.

Table 8 shows the P% for tensile strength. Hence, P% for tensile strength was zirconium dioxide 23.74%, silicon 17.07%, and processing technique 57.33%. Hence, from the ANOVA results we can conclude that the processing technique gave the maximum contribution towards compressive strength. Figure 23 shows the images of tensile strength test specimens.

Table 8. ANOVA for SN ratios.

Source	DF	Seq SS	Adj SS	Adj MS	F	P	P (%)
(A) Processing technique	1	30.52	30.52	30.52	296.1	0.000	57.33
(B) Silicon (wt.%)	3	27.26	27.26	9.088	88.1	0.000	17.07
(C) Zirconium dioxide (wt.%)	3	37.86	37.85	12.61	122.4	0.000	23.74
AXB	3	0.126	0.126	0.042	0.41	0.750	0.08
AXC	3	0.367	0.366	0.122	1.19	0.369	0.29
BXC	9	7.178	7.177	0.797	7.74	0.003	1.49
Residual error	9	0.928	0.927	0.103			
Total	31	104.25					

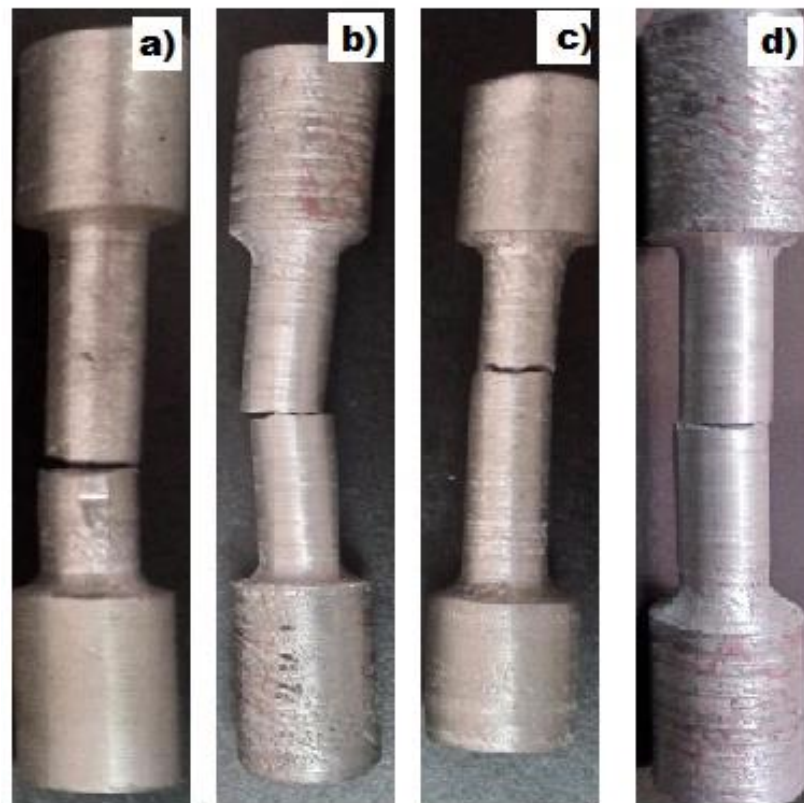


Figure 23. Tensile strength test specimens of spray forming processing techniques of Si-Al alloy matrix reinforced with (a) 0% (b) 5% (c) 10% (d) 15% ZrO_2 particulates for 13 wt.% Si.

Figure 24a–c shows the SEM images of the fracture surface of Si-Al- ZrO_2 (5, 10, 15 wt.%) composites. From Figure 25a for Si-Al- ZrO_2 (5 wt.%) composite, it is observed that ZrO_2 particulates resulted in multiple crack propagation, whereas in the case of Si-Al- ZrO_2 (10, 15 wt.%) composite, shown in Figure 25b,c, ZrO_2 particle distribution is greater which results in reduction in crack and void formation.

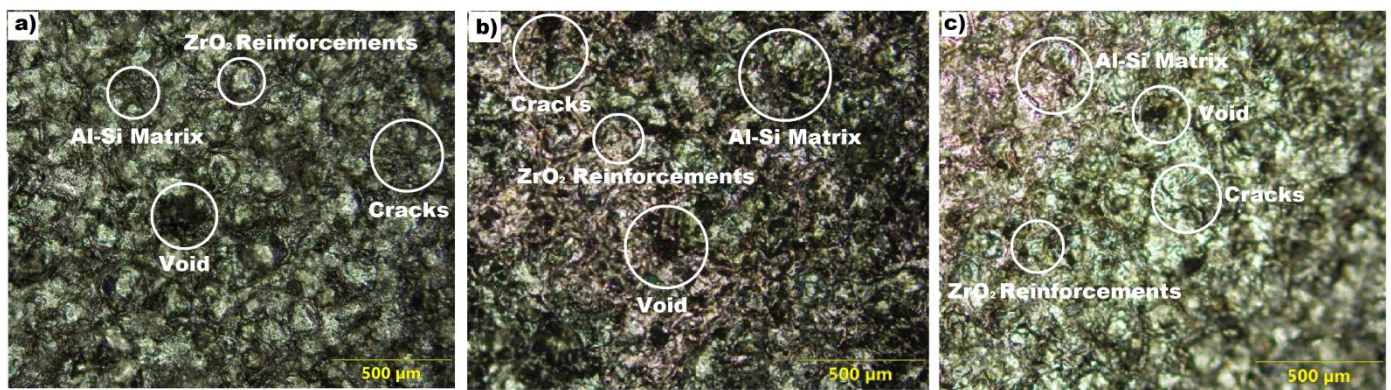


Figure 24. SEM images of fracture surface of (a) Si-Al-ZrO₂ (5 wt.%); (b) Si-Al-ZrO₂ (10 wt.%); (c) Si-Al-ZrO₂ (15 wt.%) for 13 wt.% Si (surface perpendicular to the direction of loading).

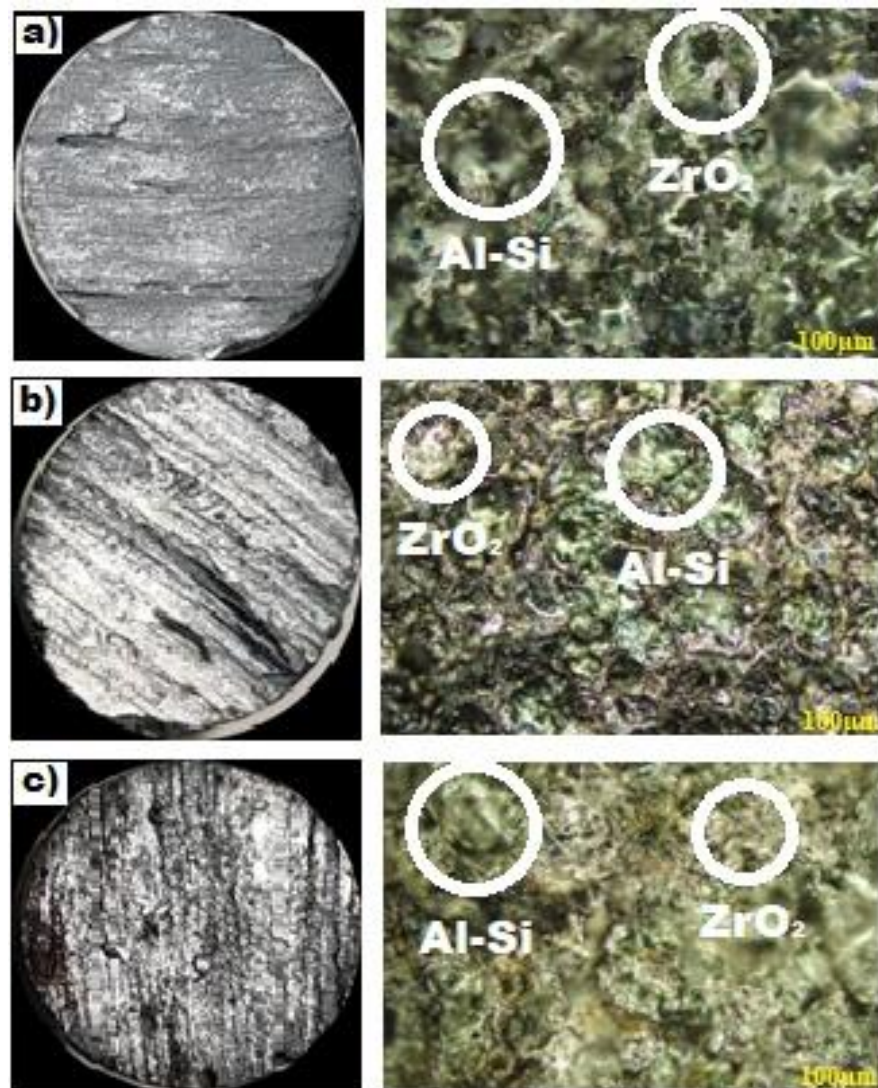


Figure 25. Microstructural changes of Si-Al (13 wt.% Si) (a) ZrO₂ (5 wt.%), load (19.62 N), and sliding speed (1.67 m/s); (b) ZrO₂ (10 wt.%), load (19.62 N), and sliding speed (1.67 m/s); (c) ZrO₂ (15 wt.%), load (19.62 N), and sliding speed (1.67 m/s).

3.4. Wear

Wear rate of the Si-Al alloy matrix reinforced with ZrO₂ particulates composites under different wear conditions, load (L/N), sliding speed (m/s), and ZrO₂ wt.% using L₂₇orthogonal array to decrease wear was investigated. In the influence of sliding speed on the wear rate of the 5 wt.%, 10 w.%, 15 wt.% Si-Al (13 wt.% Si) alloy matrix reinforced with ZrO₂ particulates composites, it was observed that wear rate increases with sliding speed because at higher sliding speed, the temperature increases, which results in thermal softening, particle pullout, and fracture. It was also observed that the abrasive wear rate decreases with addition of ZrO₂ wt.% with minimum particle pullout under all testing condition. Thus, it can be concluded that addition of the ZrO₂ wt.% in the Si-Al alloy matrix improves its wear resistance. Finally, the influence of load, i.e., 19.62 N on the abrasive wear rate of Si-Al alloy matrix reinforced with ZrO₂ particulates composites resulted in minimum wear. This may be due to optimum hardness values and particle debonding in Si-Al alloy matrix reinforced with ZrO₂ particulates composites. Figure 26 shows the microstructural changes for different wt.% ZrO₂ particulates under load (19.62 N) and sliding speed (1.67 m/s). From the main effects plot for SN ratios and means (Figure 27) for wear, the selection of load (19.62 N), sliding speed (1.67 m/s), and ZrO₂ (wt.%) (15 wt.%) is the best combination to get lesser wear value for Si-Al alloy matrix reinforced with ZrO₂ particulates composites.

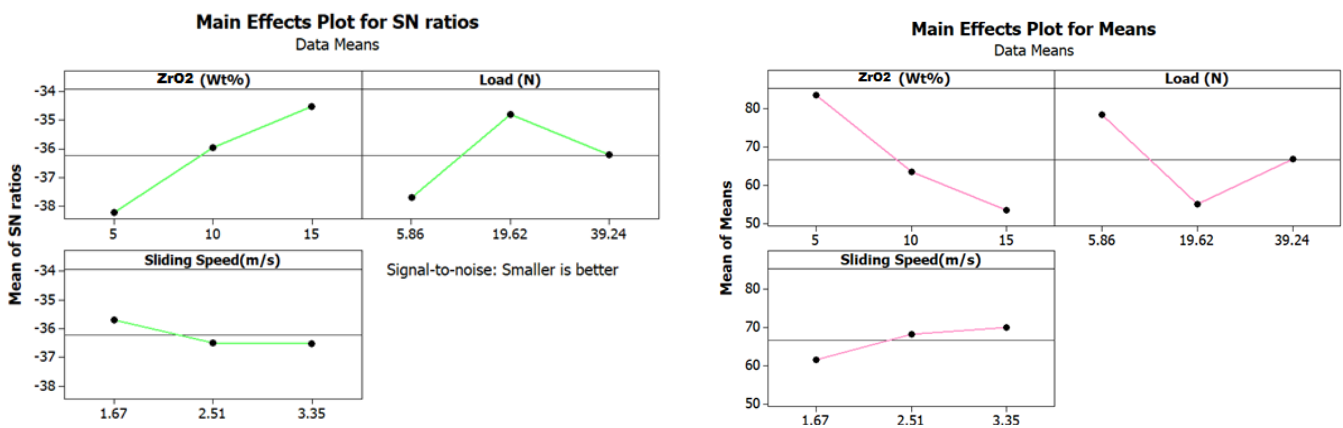


Figure 26. Mean S/N graph and mean of means for wear.

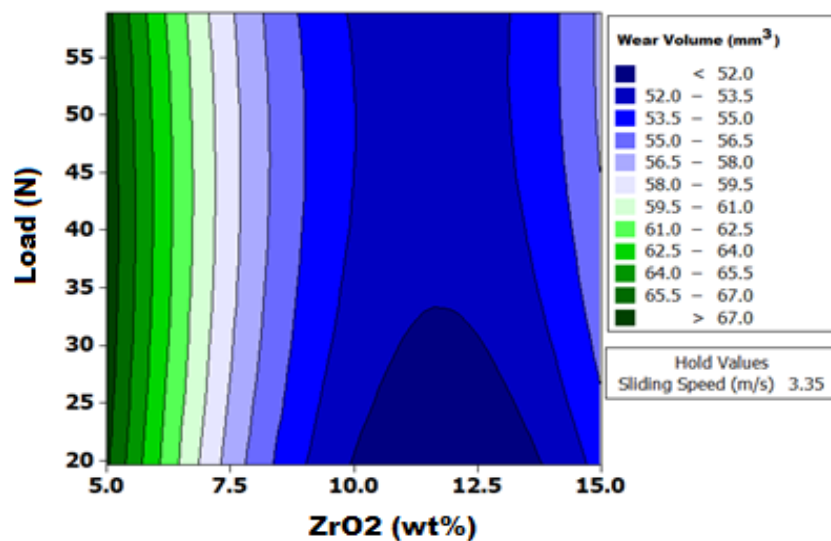


Figure 27. Contour plot for wear (mm³) V/s ZrO₂ (wt.%).

From Table 9 for percentage contribution (P%), it can be seen that ZrO₂ (wt.%) and load (N) had the maximum contribution of about 66.9% and 32.7%. Thus, load (L/N) and ZrO₂ (wt.%) are prominent parameters.

Table 9. Analysis of variance for S/N ratio.

Source	DF	Seq SS	Adj SS	Adj MS	F	P	P%
ZrO ₂ (wt.%)	2	35.2493	35.2493	17.6247	391.29	0.003	66.9
Load (N)	2	17.2316	17.2316	8.6158	191.28	0.005	32.7
Sliding Speed (m/s)	2	0.1903	0.1903	0.0951	2.11	0.321	0.4
Residual Error	2	0.0901	0.091	0.0450			
Total	8	52.7613					

Further, a second-order model was established for wear using response surface methodology.

$$\text{Wear volume (mm}^3\text{)} = 68.1004 - 7.36646A + 0.197738B + 17.2887C + 0.350909A^2 - 0.00188929B^2 - 2.44795C^2 + 0.00637105AB - 0.327381AC - 0.0227537BC + \varepsilon \quad (2)$$

From the contour plot (Figure 27), we can observe that 10 to 12.5 ZrO₂ wt.% and load of 19.62 N gave the minimum wear value for Si-Al alloy matrix reinforced with ZrO₂ particulates composites.

3.5. Electrode Wear

The electrode wear rate (EWR) is the most significant factor in electric discharge machining of Si-Al alloy matrix reinforced with ZrO₂ particulates composites and is considered electrode material removed from the workpiece under the machining time. The present study is based on ERW for Si-Al (13 wt.%) alloy matrix reinforced with ZrO₂ particulates composites by electric discharge machining under Taguchi’s L₂₇orthogonal array. Since the tool and workpiece are regarded as a set of electrodes in EDM, the electrode wear process is relatively similar to the material removal mechanism. Four different forms of EDM electrode wear may be distinguished: (a) volumetric, (b) corner, (c) end, and (d) side. Corner wear has a direct impact on cavity geometry. Maximum wear can be seen. The corners of the electrodes experienced maximum wear. One of the primary goals in the electrode design process has always been the reduction of electrode wear. For addressing electrode wear in EDM, researchers have proposed a number of solutions. The most typical machining technique suggested by researchers to compensate for tool wear is orbiting of the electrode with respect to the workpiece. It includes moving the electrode tool in a planetary motion that produces a powerful flushing action, increasing the precision of the component and the process efficiency [21–23]. From the experimental investigation using main effects plot for electrode wear under electric discharge machining of Si-Al (13 wt.%) alloy matrix reinforced with ZrO₂ particulates composites, it was observed that at maximum peak current of 12 Amps, pulse on time of 300 μs, pulse off time 150 μs, 15 wt.% ZrO₂ particulates using graphite electrode, the electrode wear was affected by the carbon precipitation from dielectric fluid on the electrode surface. Further, rapid wear on the electrode edge due to the failure of carbon to precipitate was also observed.

Further, with copper as an electrode, ZrO₂ 10 wt.%, and minimum peak current(8A), the wear of the electrode is reduced. Experiments based on Taguchi’s design of experiments, i.e., L₂₇orthogonal array is used for further analysis of EWR under different machining conditions of Si-Al alloy matrix reinforced with ZrO₂ particulates composites. Figure 28 shows the Variation of EWR (mm³/min) under different machining conditions. Figure 29 shows the interaction plot of EWR (mm³/min) under different machining conditions. Figure 30a–c shows the microstructural changes of Si-Al alloy matrix reinforced with 5, 10 and 15 wt.% ZrO₂ particulates composites respectively under different conditions. Further,

Figure 31a–c shows the microstructural changes in Brass, Copper and Graphite electrode materials respectively.

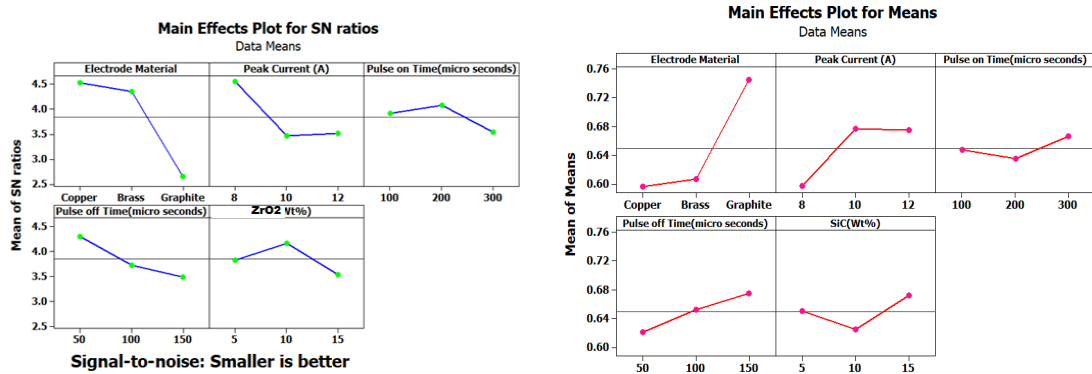


Figure 28. Variation of EWR (mm^3/min) under different machining conditions.

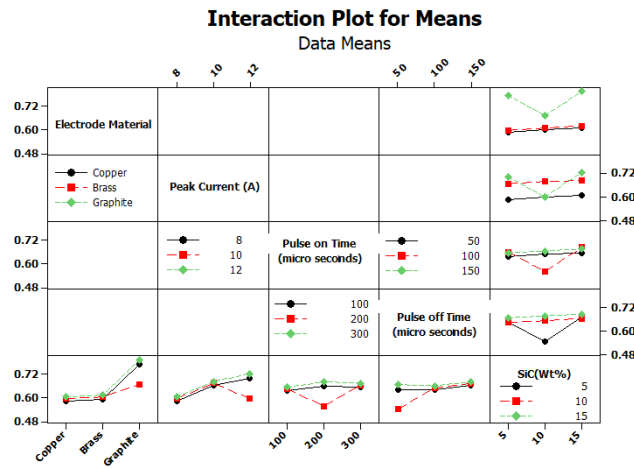


Figure 29. Interaction plot of EWR (mm^3/min) under different machining conditions.

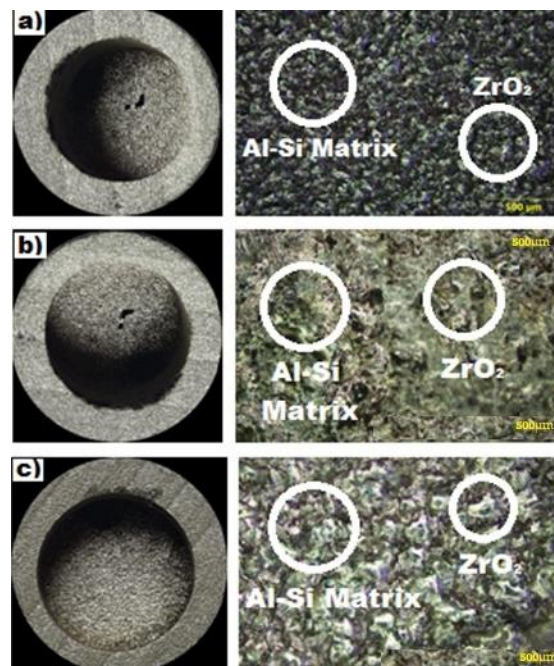


Figure 30. Microstructural changes of work piece material (a–c).



Figure 31. Microstructural changes of electrode material (a–c).

Change in surface and subsurface properties of the electrode material is found during machining of Si-Al (13 wt.% Si) alloy matrix reinforced with ZrO₂ particulates composites due to increase in temperature exceeding more than 10,000 °C and rapid quenching.

4. Conclusions

Based on processing, mechanical characterization, and machinability study on stir cast and spray formed Si-Al alloy reinforced with zirconium dioxide particulate composites, these conclusions can be reached:

- From the results, it was observed that the spray forming technique resulted in increased micro hardness due to increased barriers, dislocation density, and uniform dispersion of ZrO₂ particulates. Further increase in ZrO₂ particles resulted in decreased compressive strength. Finally, tensile strength of the composite increases with increase in the ZrO₂ particle wt.%. However, for 15 wt.% of ZrO₂ particulates and 13 wt.% Si, it can be seen that tensile strength value increases to 139.87 MPa. This may be due to larger strain hardening, dislocation tangles, homogenous distribution of particulates, grain refinement, and plastic incongruity.
- From the results obtained for wear on 5 wt.%, 10 wt.%, 15 wt.% Si-Al alloy matrix reinforced with ZrO₂ particulates composites, it was observed that wear rate increases with increasing sliding speed. This is because at higher sliding speed, the temperature increases, resulting in thermal softening, particle pullout, and fracture. It was also observed that under all test conditions, the wear rate decreased with addition of ZrO₂ wt.% with minimum particle pullout. Thus, it can be concluded that addition of the ZrO₂ wt.% in Si-Al (13 wt.% Si) alloy matrix improves its wear resistance. Finally, the influence of load, i.e., 19.62 N on the abrasive wear rate of Si-Al alloy matrix reinforced with ZrO₂ particulates composites resulted in minimum wear. This may be due to optimum hardness values and particle debonding in Si-Al alloy matrix reinforced with ZrO₂ particulates composites.
- From the experimental investigation using main effects plot for electrode wear under electric discharge machining of Si-Al (13 wt.% Si) alloy matrix reinforced with ZrO₂ particulates composites, clearly indicates that at maximum peak current of 12 Amps, pulse on time of 300 μs, pulse off time 150 μs, 15 wt.% ZrO₂ particulates using graphite electrode, the electrode wear gets affected by the carbon sedimentation from the hydrocarbon rich dielectric fluid on the surface of electrode during sparking. However, while copper is used as electrode material, electrode wear decreased.

- Change in surface and subsurface properties of the electrode material is found during machining of Si-Al (13 wt.% Si) alloy matrix reinforced with ZrO₂ particulates composites due to increase in temperature exceeding more than 10,000 °C and rapid quenching.

Author Contributions: Conceptualization, R.S., A.H. and M.S.S.A.; Data curation, R.S., A.H. and M.S.S.A.; Formal analysis, R.S., A.H. and I.S.P.; Investigation, R.S., A.H. and I.S.P.; Methodology, R.S. and A.H.; Project administration, R.S.; Resources, R.S. and N.N.; Software, J.H. and A.H.; Supervision, R.S., N.N. and M.N.; Validation, R.S., J.H. and I.S.P.; Visualization, J.H.; Writing—original draft, R.S., A.H., M.S.S.A. and M.N.; Writing—review & editing, R.S., P.R.G., J.H., A.H., M.S.S.A., I.S.P. and M.N. All authors have read and agreed to the published version of the manuscript.

Funding: This research received no external funding.

Data Availability Statement: Data are available upon request.

Acknowledgments: Authors would like to acknowledge Manipal Institute of Technology, Manipal, Karnataka, 576104, India for providing support for carrying out experimentations.

Conflicts of Interest: The authors declare no conflict of interest.

References

1. Navuluri, V.K.; Bellamkonda, P.N.; Sudabathula, S. Characterization of Graphite and Zirconium dioxide on Al-7075 Metal Matrix Composites (MMCS) Fabricated by Stir Casting Technique. *Int. J. Trend Sci. Res. Dev.* **2019**, *3*, 820–823. [[CrossRef](#)]
2. Ramachandra, M.; Abhishek, A.; Siddeshwar, P.; Bharathi, V. Hardness and Wear Resistance of ZrO₂ Nano Particle Reinforced Al Nanocomposites Produced by Powder Metallurgy. *Procedia Mater. Sci.* **2015**, *10*, 212–219. [[CrossRef](#)]
3. Anjaneyulu, B.; Rao, G.N.; Rao, K.P. Development, mechanical and tribological characterization of Al₂O₃ reinforced ZrO₂ ceramic composites. *Mater. Today Proc.* **2020**, *in press*. [[CrossRef](#)]
4. Kumar, V.R.; Pramod, R.; Sekhar, C.G.; Kumar, G.P.; Bhanumurthy, T. Investigation of physical, mechanical and tribological properties of Al6061–ZrO₂ nano-composites. *Heliyon Conf. Ser.* **2019**, *5*, e02858. [[CrossRef](#)] [[PubMed](#)]
5. Abd-Elwahed, M.; Ibrahim, A.; Reda, M. Effects of ZrO₂ nanoparticle content on microstructure and wear behavior of titanium matrix composite. *J. Mater. Res. Technol.* **2020**, *9*, 8528–8534. [[CrossRef](#)]
6. Khalili, V.; Heidarzadeh, A.; Moslemi, S.; Fatheyunes, L. Production of Al6061 matrix composites with ZrO₂ ceramic reinforcement using a low-cost stir casting technique: Microstructure, mechanical properties, and electrochemical behavior. *J. Mater. Res. Technol.* **2020**, *9*, 15072–15086. [[CrossRef](#)]
7. Pandiyarajan, R.; Maran, P.; Marimuthu, S.; Ganesh, K.C. Mechanical and tribological behavior of the metal matrix composite AA6061/ZrO₂/C. *J. Mech. Sci. Technol.* **2017**, *31*, 4711–4717. [[CrossRef](#)]
8. Thandalam, S.K.; Ramanathan, S.; Sundarrajan, S. Synthesis, microstructural and mechanical properties of ex situ zircon particles (ZrSiO₄) reinforced Metal Matrix Composites (MMCs). *J. Mater. Res. Technol.* **2015**, *4*, 333–347. [[CrossRef](#)]
9. Karthikeyan, G.R.; Jinu, G. Experimental investigation on mechanical and wear behaviour of Aluminum LM6/ZrO₂ Composite Fabricated by Stir casting method. *J. Balk. Tribol. Assoc.* **2015**, *21*, 539–556.
10. Manjunatha, B.R.; Anil Kumar, A. Mechanical Characterization of Al6061/ZrO₂/Zirconium dioxide Sand Hybrid Metal Matrix Composite. *Int. J. Eng. Res. Technol. (IJERT)* **2016**, *4*, 1–5.
11. Udayashankar, S.; Ramamurthy, V.S. Development and Characterization of Al6061-Zirconium dioxide Reinforced Particulate Composites. *Int. J. Eng. Technol.* **2018**, *7*, 128.
12. Rengasamy, N.; Rajkumar, M.; Kumaran, S.S. An analysis of mechanical properties and optimization of EDM process parameters of Al 4032 alloy reinforced with ZrB₂ and TiB₂ in-situ composites. *J. Alloys Compd.* **2016**, *662*, 325–338. [[CrossRef](#)]
13. Srinivasan, R.; Pridhar, T.; Kirubakaran, R.; Ramesh, A. Prediction of wear strength of squeeze cast Aluminum hybrid Metal Matrix Composites using Response Surface Methodology. *Mater. Today Proc.* **2020**, *in press*. [[CrossRef](#)]
14. Umanath, K.; Palanikumar, K.; Sankaradass, V.; Uma, K. Optimization of wear properties on AA7075/SiC/MoS₂ hybrid metal matrix composite by Response Surface Methodology. *Mater. Today Proc.* **2020**, *46*, 4019–4024. [[CrossRef](#)]
15. Bachchhav, B.; Naranje, V. Effect of high volume fraction reinforcement on electro-discharge machining of Al-Al₂O₃ MMC. *Mater. Today Proc.* **2020**, *in press*. [[CrossRef](#)]
16. Lee, C.-S.; Heo, E.-Y.; Kim, J.-M.; Choi, I.-H.; Kim, D.-W. Electrode Wear Estimation Model for EDM Drilling. In *Robotics and Computer-Integrated Manufacturing*; Elsevier: Amsterdam, The Netherlands, 2015; Volume 36, pp. 70–75, ISSN 2278-0181.
17. Hou, S.; Bai, J. Experimental investigation on electrode wear of array holes machining in micro-EDM. *CIRP Manuf. Syst. Conf.* **2019**, *95*, 527–532. [[CrossRef](#)]
18. Kathiresan, M.; Sornakumar, T. EDM Studies on Aluminum Alloy-Silicon Carbide Composites Developed by Vortex Technique and Pressure Die Casting. *J. Miner. Mater. Charact. Eng.* **2010**, *9*, 79–88. [[CrossRef](#)]
19. Shetty, R.; Pai, R.; Barboza, A.B.; Shetty, Y. Statistical and Surface Metallurgical Study During Electric Discharge Machining of Ti-6Al-4V. *ARPN J. Eng. Appl. Sci.* **2018**, *13*, 3594–3600.

20. Shetty, R.; Pai, R.B.; Rao, S.S.; Kamath, V. Machinability study on discontinuously reinforced Aluminum Composites (DRACs) using Response Surface Methodology and Taguchi's design of experiments under dry cutting condition. *Maejo Int. J. Sci. Technol.* **2008**, *2*, 227–239.
21. Shetty, R.; Pai, R.B.; Rao, S.S.; Kamath, V. Taguchi's Technique in Machining of Metal Matrix Composites. *J. Braz. Soc. Mech. Sci. Eng.* **2009**, *31*, 12–20. [[CrossRef](#)]
22. Shetty, R.; Hegde, A. Taguchi based fuzzy logic model for optimization and prediction of surface roughness during AWJM of DRCUFP composites. *Manuf. Rev.* **2022**, *9*, 2.
23. Karthik, S.R.; Londe, N.V.; Shetty, R.; Nayak, R.; Hedge, A. Optimization and prediction of hardness, wear and surface roughness on age hardened stellite 6 alloys. *Manuf. Rev.* **2022**, *9*, 10.